Ultrasound in Med. & Biol. Vol. 17, No. 3, pp. 257–263, 1991
Printed in the U.S.A.

0301-5629/91 $3.00 + .00

●*Original Contribution*

IN SITU EXPOSIMETRY: THE OVARIAN ULTRASOUND EXAMINATION

TARIQ A. SIDDIQI,† WILLIAM D. O'BRIEN, JR.,‡ RICHARD A. MEYER,*
JOAN M. SULLIVAN† and MENACHEM MIODOVNIK†

†University of Cincinnati College of Medicine, Department of Obstetrics and Gynecology, 231 Bethesda Avenue, Cincinnati, OH 45267-0526, USA;
‡University of Illinois at Urbana-Champaign, Department of Electrical and Computer Engineering, 1406 West Green Street, Urbana, IL 61801, USA;
*Children's Hospital Medical Center, Division of Cardiology, Elland and Bethesda Avenues, Cincinnati, OH 45229, USA

(*Received* 19 *July* 1990; *in final form* 24 *October* 1990)

Abstract—We have constructed a specialized *in vivo* exposimetry system and developed and tested customized software using specially fabricated hydrophones. We placed the hydrophones in the lateral vaginal fornix as close to the ovary as possible (usually 1–2 cm from the ovary) and determined selected first-order and second-order ultrasonic field quantities during a routine ultrasound examination of the ovary. Our sonographic measurements yielded mean ultrasound beam path distances of 7.6 cm. (n = 18) in the presence of a distended bladder and 7.0 cm. (n = 25) in the presence of an empty bladder with an average group insertion loss of 6.2 dB and 7.3 dB, respectively. Using a Fixed Attenuation Model, the tissue attenuation coefficient value was 2.98 dB/MHz; whereas for the Overlying Tissue Model the value was 0.72 dB/cm-MHz. These data are both specific and unique in that they have been systematically obtained *in situ*.

Key Words: **Ultrasound, Exposimetry, *In situ*.**

INTRODUCTION

Although ultrasound irradiation is known to produce bioeffects in experimental animals (O'Brien 1984; O'Brien 1991), the available experimental data for the reproductive sciences for threshold levels of ultrasound that induce lethal and nonlethal abnormalities are very limited. As a partial first step, it is critical to determine the actual ultrasonic energy imparted to the human ovary, embryo and early fetus during a diagnostic ultrasound examination in order to provide the basis to extrapolate animal studies to humans.

In this first of a series of planned and ongoing *in vivo* human exposimetry studies, we report the selected first-order and second-order ultrasonic field quantities to which the human ovary is exposed during the course of a "routine" diagnostic ultrasound examination. First-order ultrasonic quantities include (1) the pressure waveform, (2) the maximum value of the peak compressional pressure and (3) the maximum value of the peak rarefactional pressure. Second-order quantities include (1) spatial peak, temporal average intensity, (2) spatial peak, pulse average intensity and (3) spatial peak, temporal peak intensity.

We tested the hypothesis that *in vivo* ultrasound exposure of the ovary during a diagnostic ultrasound examination is several orders of magnitude less than the maximum values of ultrasonic quantities measured *in vitro;* and that patient size is directly related to the amount of ultrasound radiation to which the ovary is exposed.

METHODS

Diagnostic imaging system

A 3.0 MHz frequency, mechanical sector transducer (focal zone 5.5–13 cm, focal point 8 cm, crystal diameter 19 mm) in combination with an ATL Ultramark 4, Model (Advanced Technology Laboratories, Botthel, WA, USA) diagnostic ultrasound imaging system was used for all studies. Exposure time after obtaining an acceptable real-time image was 5 min.

Address correspondence to: Tariq A. Siddiqi, University of Cincinnati Medical Center, 231 Bethesda Avenue, Cincinnati, OH 45267-0526, USA.

Supported in part by NIH HD21687 and HD20748.

Power setting for the instrument was 100% at all times.

Exposimetry instrumentation

The customized exposimetry equipment and software for *in vivo* and calibration studies have been previously reported in detail (Daft et al. 1990). In summary, instrumentation has been developed to measure the acoustic pressure field during a diagnostic reproductive system ultrasound examination. The ultrasonic field is sampled using a calibrated 7-element linear array hydrophone of polyvinylidene difluoride transducers, which is placed as close as possible to the ovary using real-time imaging. The RF signals from the hydrophone are digitized at 50 Ms/s and the maximum amplitude in waveform received in the examination is recorded. The reference output of the clinical real-time scanner is obtained by placing the hydrophone in a 37°C water bath at the same distance from the clinical transducer as that used to obtain the *in vivo* recording. From the hydrophone recordings, 10 exposimetry quantities were determined, five under *in vivo* conditions and five in the water tank, that is, *in vitro* conditions. The five quantities were the maximum peak compressional pressure, p_r, the maximum peak rarefactional pressure, p_r, the spatial peak, temporal peak intensity, I_{SPTP}, the spatial peak, temporal average intensity, I_{SPTA}, and the spatial peak, pulse average intensity, I_{SPPA}, (AIUM/NEMA standard; Daft et al. 1990).

Patient population

Healthy, nonpregnant female volunteers were recruited for the study. Each subject was counseled and asked to sign an informed consent statement as approved by the University of Cincinnati Medical Center Institutional Review Board. Each subject was studied only once for data analysis. The volunteers were divided into two groups: *Group A* was comprised of individuals who had a full bladder and the ultrasound beam pathway included passage through the anterior abdominal wall and distended bladder prior to visualization of the hydrophone (Figs. 1a, b). *Group B* was comprised of individuals whose bladder was empty and the ultrasound beam pathway included passage through the anterior abdominal wall and uterus/cervix prior to visualization of the hydrophone (Figs. 2a, b). Patient size thus varied depending upon the distance between the abdominal wall skin surface (transducer) and the ovary (hydrophone).

Fig. 1a. Representative sonogram from a Group A subject demonstrating anterior abdominal wall, distended bladder and hydrophone in vagina. (Lower "x" marks hydrophone.)

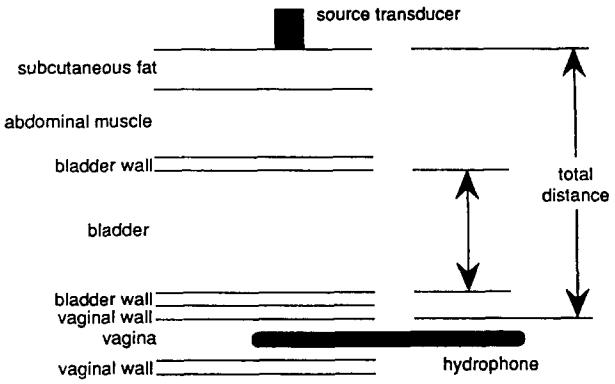

Fig. 1b. Schematic of tissue layers through which ultrasound beam passes prior to reaching hydrophone in vagina and the distances measured for Group A subjects.

Hydrophone placement and study protocol

Each subject was placed in a supine position with the hips abducted, knees flexed and externally rotated, *i.e.*, in a "frog-leg" configuration. The specially designed hydrophone was then introduced into the vagina and placed in the lateral vaginal fornix with the hydrophone tip of the linear array as close to the ovary as possible (usually 1–2 cm from the ovary). Placement was verified using real-time imaging. The lower end of the hydrophone has a recognizable round flange to ensure appropriate placement and orientation ultrasonically. The *total distance* from the transducer to the hydrophone was then measured. This measurement included the thickness of the anterior abdominal wall which was measured separately in all subjects. In Group A individuals, *bladder width, i.e.*, the width of the urinary bladder incorporated into the total distance measurement, was also determined. The walls of the urinary bladder were not included in the bladder width measurement. All measurements were made on-line using real-time ultrasound imaging.

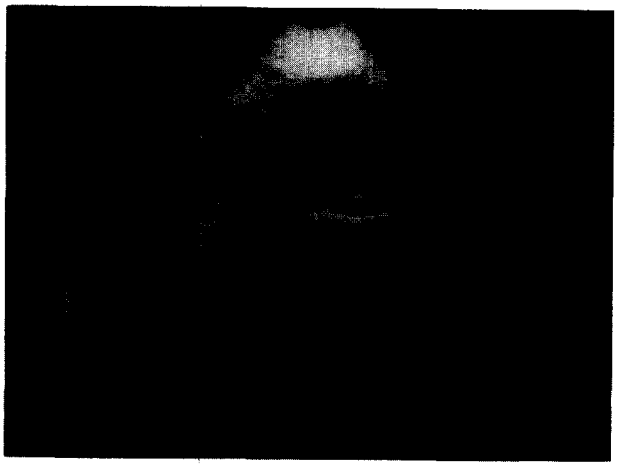

Fig. 2a. Representative sonogram from a Group B subject demonstrating anterior abdominal wall, uterus and cervix and hydrophone in vagina. Note the absence of distended bladder. (Lower "x" marks hydrophone.)

In vivo data were then obtained at 100% power settings for the diagnostic imaging system over a 5 min period. The transducer was moved across the abdominal wall surface with real-time imaging ensuring constant hydrophone visualization. The largest signal was saved for analysis (Fig. 3a). Reference data were recorded for each subject, after completion of each *in vivo* experiment, from a tank filled with water at body temperature (37°C) and with the hydrophone and transducer fixed at the same total distance as in the *in vivo* experiment. Again, the largest signal recorded over a 5 min period during each water path experiment was saved for data analysis (Fig. 3b).

Data analysis

For each study, a complete set of *in vivo* and *in vitro* pressure waveforms were obtained along with a sonogram from which tissue-path distances were measured. Six insertion loss values (loss as determined by the measurement procedure) were calculated for each complete data set, that is,

$$IL = 20 \log_{10}(\textit{in vitro} \text{ pressure}/\textit{in vivo} \text{ pressure})$$

where the pressure ratios were for p_c, p_r and $p_c + p_r$ and

$$IL = 10 \log_{10}(\textit{in vitro} \text{ intensity}/\textit{in vivo} \text{ intensity})$$

where the intensity ratios were for I_{SPTP}, I_{SPTA} and I_{SPPA}. An average insertion loss value, $\langle IL \rangle$, of the six insertion loss values represented the insertion loss value of each subject for subsequent calculations.

Two tissue models were evaluated. The fixed-attenuation tissue model (Carson 1989) is based on the assumption that the attenuation between the abdominal surface and uterus is linearly dependent upon frequency and independent of distance. The fixed-attenuation tissue model "attenuation coefficient" is calculated by dividing the average insertion loss by the center frequency f_c, that is,

$$A_{fa} = \langle IL \rangle / f_c \quad \text{(in dB/MHz)}$$

for each subject.

The overlying tissue model is based on the assumption that the attenuation consists only of that due to the intact tissue and the fluid path contributes no attenuation. The overlying tissue model "attenuation coefficient" is calculated by dividing the average insertion loss by the center frequency and the distance of the nonfluid path, d_{nf}, that is,

$$A_o = \langle IL \rangle / (f_c d_{nf}) \quad \text{(in dB/cm-MHz)}$$

for each subject.

RESULTS

The number of subjects in each group as well as the total distance from transducer to hydrophone, including abdominal wall thickness, bladder width (Group A) and uterus/cervix component (Group B), is shown in Table 1.

First-order ultrasonic quantities, *i.e.*, the peak positive pressure and the peak negative pressure for *in vivo* and *in vitro* experiments are shown in Table 2. The group insertion loss average $\langle IL \rangle_g$ in dB is also shown for both groups.

Second-order ultrasonic quantities, *i.e.*, the SPTA, SPPA and SPTP intensities are shown in Table 3 for both groups; as is the group insertion loss average $\langle IL \rangle_g$ in dB for each of the intensity measurements.

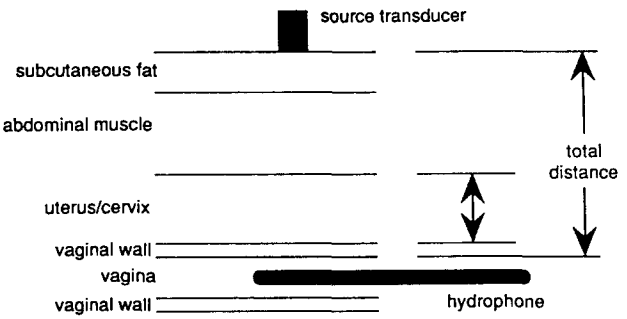

Fig. 2b. Schematic of tissue layers through which ultrasound beam passes prior to reaching hydrophone in vagina and the distances measured for Group B subjects.

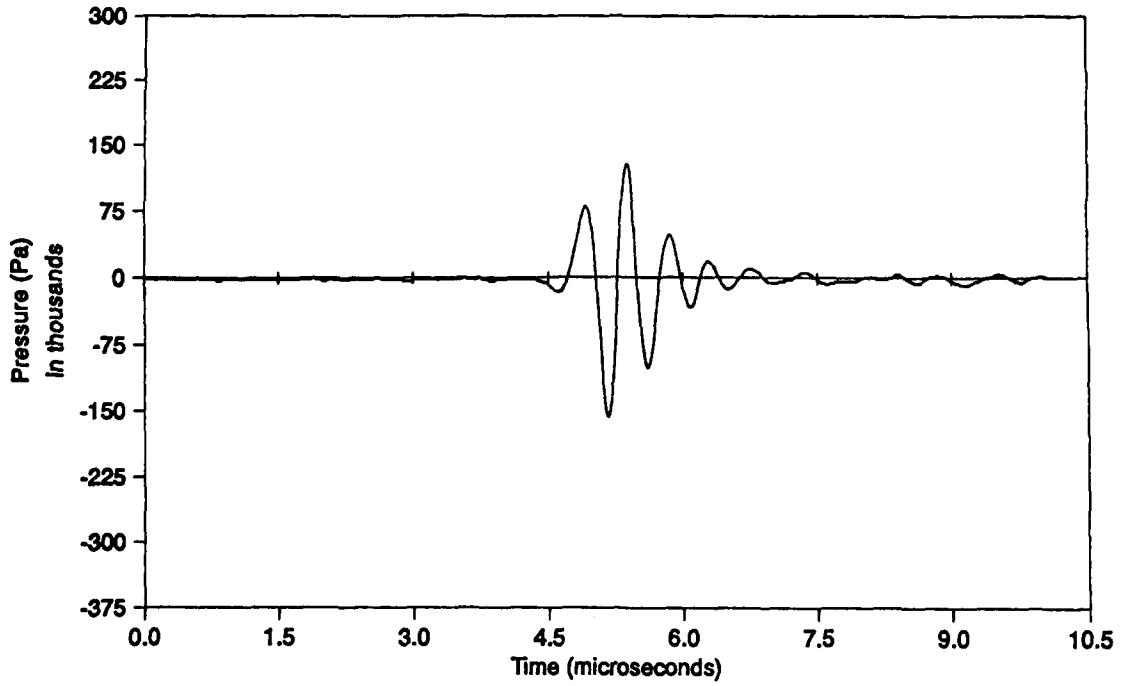

Fig. 3a. Representative example of an *in vivo* pressure waveform.

Power spectra for the *in vivo* and *in vitro* signals are plotted in Fig. 4. The peak for the *in vitro* signal recorded in the water bath is at 2.4 MHz whereas the peak for the *in vivo* spectrum is shifted down to 2.1 MHz. Since tissue attenuation is frequency dependent, the spectrum from the *in vivo* measurement is shifted down in frequency relative to the *in vitro* measurement. However, this does not explain the down-

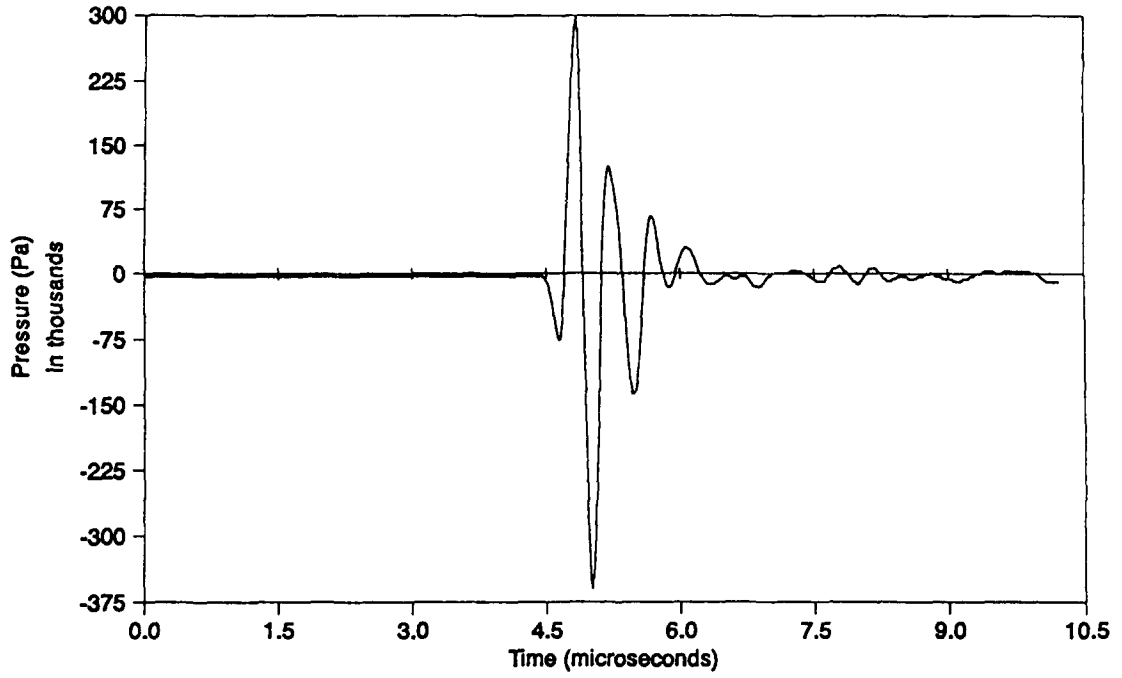

Fig. 3b. Representative example of an *in vitro* pressure waveform signal obtained in the same subject from hydrophone in water tank.

Table 1. Total distance from transducer to hydrophone including abdominal wall thickness, bladder width and uterus/cervix component for Group A (full bladder) and Group B (empty bladder) subjects expressed as mean ± standard deviation (range) in centimeters.

Group (*n*)	Abdominal wall	Bladder	Uterus/cervix	Total distance
A (18)	3.1 ± 0.9 (1.8–5.2)	4.5 ± 0.8 (3.0–6.2)	0	7.6 ± 1.3 (5.2–10.0)
B (25)	4.6 ± 1.1 (2.4–7.4)	0	2.3 ± 0.5 (1.5–3.6)	7.0 ± 1.4 (4.9–11.0)

ward shift relative to the transducer label of 3.0 MHz. For completeness, subsequent calculations which required frequency were therefore performed using both 2.1 and 2.4 MHz.

Data for insertion loss are therefore estimated at both 2.4 MHz and 2.1 MHz frequencies in the two tissue models used for further data analysis:

1. *Overlying tissue model (dB/cm-MHz)* where no attenuation is assumed to have occurred during passage through a fluid path; and
2. *Fixed-attenuation tissue model (dB/MHz)* where signal attenuation is assumed to occur uniformly across the total distance irrespective of an intervening fluid path, *e.g.*, urine in the bladder.

Data for the fixed-attenuation tissue model and for the overlying tissue model at 2.4 MHz and 2.1 MHz are shown in Table 4 along with a group insertion loss average for each group.

DISCUSSION

Diagnostic ultrasound imaging is used extensively in clinical reproductive medicine. The reproductive endocrinologist, for example, uses this modality to monitor follicular growth, development and ovulation (O'Herlihy and Ch de Crespigny 1980). This information is then used to promote fertilization and conception by either natural or artificial methods. In a similar fashion, all *in vitro* fertilization programs employ ultrasound imaging for timing surgical ovum retrieval efforts (Vargyas et al. 1982). Thus, 5–10% of all pregnancies in the United States occur as a result of fertilization of ova exposed to ultrasonic energy in the preovulatory stage, some with multiple exposures. A number of investigators have attempted to determine the effects of ultrasound related to DNA and hereditary changes in a variety of *in vivo* and *in vitro* experiments (O'Brien 1984; O'Brien 1991). The results to date are conflicting because of a lack of uniformity in experimental conditions, exposure times, ultrasound intensities employed and the endpoints measured. The spatial average, temporal average intensities in mW/cm^2 reported for pulsed-wave ultrasound experiments ranges from less than 0.2 to 200 W/cm^2 and the total exposure time in these experiments ranges from 1 min to 90 min (Stewart et al. 1985). A large number of these investigations have been directed towards measuring the rate of sister chromatid exchange in human lymphocyte cultures although different laboratories have reported both positive and negative results (Goss 1984). Other observations related to DNA and hereditary changes include decreased incorporation of DNA precursor (Prasad et al. 1976), unscheduled non-S-phase DNA synthesis (Liebeskind et al. 1979), and hereditary changes in cell mobility (Liebeskind et al. 1982). Testart et al. (1982) observed premature ovulation in 5 out of 23 and 8 out of 19 cycles when ultrasonography occurred in the three days preceding or in the 36 h following ovulatory stimulus, respectively. Despite this voluminous literature, there appears to be no information available with respect to the actual ultrasonic energy exposure to the human ovary during a routine, clinical ovarian examination.

There have been a few studies, summarized by Stewart and Stratmeyer (1982) and the National Council on Radiation Protection (NCRP) (1983), which estimate the ultrasonic attenuation in tissues overlying the first trimester embryo. However, this is the first known report relative to estimating the exposure to the ovary although the previously reported studies provide a basis for comparison.

In a summary of five studies (Stewart and Stratmeyer 1982), distances between the abdominal sur-

Table 2. Peak positive (P_c) and peak negative pressures (P_r) in megapascals (MPa) for *in vivo* and *in vitro* experiments including the group insertion loss average $\langle IL \rangle_g$ in decibels (dB) for Group A and Group B subjects expressed as mean ± standard deviation (range).

Group (*n*)	*In vivo* P_c (MPa)	*In vitro* P_c (MPa)	Avg $\langle IL \rangle_g$ (dB)	*In vivo* P_r (MPa)	*In vitro* P_r (MPa)	Avg $\langle IL \rangle_g$ (dB)
A (18)	0.2 ± 0.1 (0.04–0.3)	0.4 ± 0.2 (0.06–0.6)	6.4 ± 4.1 (2.3–27.1)	0.2 ± 0.1 (0.02–0.3)	0.4 ± 0.2 (0.1–0.8)	6.1 ± 3.4 (2.1–21.2)
B (25)	0.1 ± 0.07 (0.04–0.3)	0.3 ± 0.1 (0.06–0.6)	7.8 ± 5.5 (2.3–27.1)	0.2 ± 0.08 (0.02–0.3)	0.3 ± 0.2 (0.1–0.8)	6.9 ± 4.7 (2.1–21.2)

Table 3. Second-order ultrasonic quantities including SPTA, SPPA and SPTP and group insertion loss average $\langle IL \rangle_g$ in dB for Group A and Group B subjects expressed as mean ± standard deviation (range).

Group	*In vivo* SPTP (W/cm^2)	*In vitro* SPTP (W/cm^2)	Avg $\langle IL \rangle_g$ (dB)	*In vivo* SPTA (mW/cm^2)	*In vitro* SPTA (mW/cm^2)	Avg $\langle IL \rangle_g$ (dB)	*In vivo* SPPA (W/cm^2)	*In vitro* SPPA (W/cm^2)	Avg $\langle IL \rangle_g$ (dB)
A (18)	4.2 ± 4.4 (0.1–17.8)	16.0 ± 18.5 (3.1–82.5)	6.1 ± 3.5 (0.07–13.4)	3.8 ± 4.0 (0.2–12.9)	10.9 ± 8.2 (2.3–29.4)	5.7 ± 3.1 (0.8–11.5)	0.6 ± 0.6 (0.02–2.1)	3.0 ± 4.8 (0.4–21.2)	6.3 ± 3.8 (0.7–13.3)
B (25)	2.1 ± 2.0 (0.02–8.0)	10.1 ± 10.3 (0.6–43.6)	7.1 ± 4.7 (2.0–21.6)	1.9 ± 1.8 (0.2–6.8)	8.0 ± 8.1 (0.6–33.9)	6.1 ± 3.7 (1.7–15.1)	0.3 ± 0.3 (0.08–1.0)	1.6 ± 1.7 (0.1–7.7)	7.4 ± 4.9 (2.0–24.2)

face and the uterine cavity in early pregnancy ranged between 2 and 11 cm. Using a worst-case approach (Carson et al. 1989), similar distance was estimated to be 2.6 cm. Sonographic measurements shown in Table 1 yielded distances between the abdominal surface and the vagina between 4.9 and 11.0 cm with means of 7.6 cm for the distended bladder group and 7.0 cm for the empty bladder group. These results are consistent with Stewart and Stratmeyer's (1982) summary. However, there is considerable disagreement with the estimated worst-case approach of Carson et al. (1989) where we measured the absolute minimum distance to be about twice as great as their estimated minimum distance.

To quantify the loss of the ultrasonic signal between the abdominal surface and either the uterine cavity or vagina, two terms have been utilized, *viz.*, attenuation and insertion loss. Attenuation generally implies the loss is due to tissue attenuation properties whereas insertion loss generally implies loss as determined by the measurement procedure. In general, insertion loss yields a larger value than does attenuation because the measurement takes into account loss not only due to tissue but also that due to beam diffraction and other anomalous behaviors of the beam as it propagates. In our case, we explicitly mean insertion loss because it was calculated directly from the *in vivo* and *in vitro* measurements. In the Stewart and Stratmeyer (1982) summary, they reported the loss as attenuation with a range from 2 to 12 dB for the 2 and 2.25 MHz frequencies, although some of the reports they summarized calculated the loss from the measurement procedure. Carson et al., (1989) on the other hand, represented the loss based on tissue attenuation and estimated the attenuation to be 3.9 dB at 3.5 MHz. Another calculation (Table 2.4 in NCRP 1983), also based on tissue attenuation, estimated the attenuation to be 4.1 dB at 3.5 MHz. The 3.9 and 4.1 dB estimates were based on worst-case modeling and thus were lower than ours by about 3 dB. Stewart and

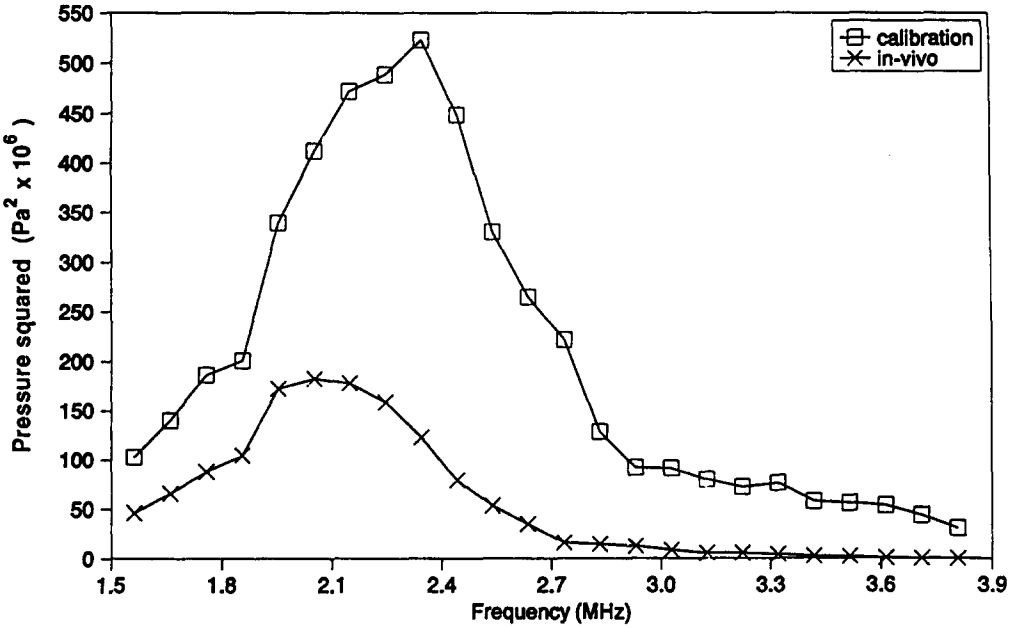

Fig. 4. Power spectra of *in vivo* and *in vitro* signals. Note that the peak for the *in vitro* signal is at 2.4 MHz whereas the peak for the *in vivo* spectrum is shifted down to 2.1 MHz.

Table 4. Group insertion loss average $\langle IL \rangle_g$ for Group A and Group B subjects in dB; attenuation coefficient (A_{fa} = insertion loss/frequency) in dB/MHz in the fixed-attenuation model in Group A subjects; attenuation coefficient (A_o = insertion loss/nonfluid path-frequency) in dB/cm-MHz in the overlying tissue model for Group A and Group B. All values are expressed as mean ± standard deviation (range) and calculated for 2.1 and 2.4 MHz frequency.

Group	Avg $\langle IL \rangle_g$ (dB)	A_{fa} (2.1 MHz) (dB/MHz)	A_{fa} (2.4 MHz) (dB/MHz)	A_o (2.1 MHz) (dB/cm-MHz)	A_o (2.4 MHz) (dB/cm-MHz)
A (18)	6.2 ± 3.5	2.98 ± 1.68	2.56 ± 1.47	1.02 ± 0.81	0.89 ± 0.71
	(0.3–13.6)	(0.14–6.47)	(0.12–5.66)	(0.06–3.60)	(0.05–3.15)
B (25)	7.3 ± 4.9			0.52 ± 0.37	0.45 ± 0.32
	(1.7–23.6)			(0.08–1.75)	(0.07–1.53)
Overall	6.7 ± 4.2			0.72 ± 0.62	0.65 ± 0.54
(43)	(0.3–23.6)			(0.08–3.60)	(0.07–3.15)

Stratmeyer's (1982) range fell within all of the values. In general, all of these loss values appeared to be consistent.

The mean values for the fixed-attenuation tissue model's attenuation coefficient are about a factor of 3 greater than the values proposed to model the attenuation coefficient for fetal exposures (Carson 1989). However, Carson (1989) was considering worst-case modeling for purposes of estimating temperature rise whereas our values represent average values. If our values are decreased about one standard deviation unit to approximate a worst-case situation, then they would closely approximate Carson's suggested value of 1 dB/MHz. Therefore, the approaches appear to yield similar values.

However, the mean values for the overlying tissue model's attenuation coefficient are approximately consistent with the attenuation coefficients of typical tissues of 0.5–1 dB/cm-MHz. The Center for Devices and Radiological Health (CDRH) of the FDA uses a value of 0.3 dB/cm-MHz as a derating factor for manufacturers to estimate ultrasonic intensity quantities in tissue. Our values are about a factor of 2 greater than the CDRH value but the CDRH value is intended to be a worst case for estimating tissue attenuation whereas our value is the average value. Therefore, given the different approaches, there is consistency. In the case of the overlying tissue model, the amount of ultrasound exposure to the ovary is dependent upon patient size, *i.e.,* the distance between the ultrasound transducer and the ovary.

In summary, it is necessary to develop a firm data base from which various modeling approaches can be explored. In our approach, we have attempted to provide mean and distribution of applicable data. It is left to the wisdom of those who wish to model *in situ* exposures to apply whatever conservatism they deem necessary in the development of exposure-based standards. Our measurements appear to be consistent with the available data bases when the different approaches are taken into account.

REFERENCES

AIUM/NEMA safety standard for diagnostic ultrasound equipment. J. Ultrasound Med. 2 (Suppl.): 1052; 1983.

Carson, P. L. Constant soft tissue distance model in pregnancy. Ultrasound Med. Biol. 15:27–29; 1989.

Carson, P. L.; Rubin, J. N.; Chiang, E. H. Fetal depath and ultrasound path lengths through overlying tissues. Ultrasound Med. Biol. 15:629–639; 1989.

Daft, C. M. W.; Siddiqi, T. A.; Fitting, D. W.; Meyer, R. A.; O'Brien, W. D., Jr. *In vivo* fetal ultrasound exposimetry. IEEE Tran. Ultrasonics, Ferroelectrics, and Frequency Control 37(6):501–505; 1990.

Goss, S. A. Sister chromatid exchange and ultrasound. J. Ultrasound Med. 3:463–470; 1984.

Liebeskind, D.; Bases, R.; Elequin, F.; Neubort, S.; Leifer, R.; Goldberg, R.; Koenigsberg, M. Diagnostic ultrasound: Effects on the DNA and growth patterns of animal cells. Radiology 131:177–184; 1979.

Liebeskind, D.; Padawer, J.; Wolley, R. et al. Diagnostic ultrasound: Time-lapse and transmission electron microscopic studies of cells isolated *in vitro.* Br. J. Cancer 45(5)(Suppl.):176–186; 1982.

National Council on Radiation Protection (NCRP). Biological effects of ultrasound: Mechanisms and clinical implications. NCRP Report No. 74. Bethesda, MD: National Council on Radiation Protection and Measurement: 1983.

O'Brien, W. D., Jr. Safety of ultrasound with selected emphasis for obstetrics. Seminars in Ultrasound 5:105–120; 1984.

O'Brien, W. D., Jr. Ultrasound bioeffects related to obstetrical sonography. In: Fleischer, A. C.; James, A. E.; Jeanty, P.; Manning, F.; Romero, R. E., eds. The principles and practice of ultrasonography in obstetrics and gynecology, fourth edition. Norwalk, CT: Appleton and Lange; 1991:15–23.

O'Herlihy, C. O.; Ch de Crespigny, L. J. Monitoring ovarian follicular development with real-time ultrasound. Br. J. Obstet. Gynaec. 87:613–618; 1980.

Prasad, N.; Prasad, R.; Bushong, S. C.; North, L. B.; Rhe, E. Ultrasound and mammalian DNA. Lancet. 1:1181; 1976.

Stewart, H. D.; Stewart, H. F.; Moore, M., Jr.; Garry, J. Compilation of reported biological effects data and ultrasound exposure levels. J. Clin. Ultrasound. 13:167–186; 1985.

Stewart, H. F.; Stratmeyer, M. E., eds. An overview of ultrasound: Theory, measurement, medical applications and biological effects. Washington, D.C.: U.S. Government Printing Office, Health and Human Services Publication (FDA); 1982:82–8190.

Testart, J.; Inserm, U.; Thiebault, A.; Frydman, R. Premature ovulation after ovarian ultrasonography. Br. J. Obstet. Gynaec. 89:694–700; 1982.

Vargyas, J. M.; Marrs, R. P.; Kletzky, O. A.; Mishell, D. R., Jr. Correlation of ultrasonic measurement of ovarian follicle size and serum estradiol levels in ovulatory patients following clomiphene citrate for *in vitro* fertilization. Am. J. Obstet. Gynecol. 144(5):569–573; 1982.